

Rendering of Japanese Artcraft

Roman Ďurikovič, Kostantin Kolchin, and Sergey Ershov ^a

Computer Graphics Laboratory, Software Department, The University of Aizu,
Ikki-machi, Aizuwakamatsu-shi, Fukushima, 965 8580 Japan.

email: {roman,kvkol}@u-aizu.ac.jp

^aKeldysh Institute for Applied Mathematics, Moscow 125047, Russia

email: measure@spp.keldysh.ru

Abstract

We present several methods for simulation of Japanese lacquer ware, a prominent Far East Asian handicraft art. We consider two most popular kinds of Japanese lacquer ware made by the makie and nashiji techniques. For rendering makie, we propose a method for preparing RGBA textures from digital photos of art items. The alpha channels of these textures control the weight with which color channels are blended with the measured bidirectional reflectance distribution function (BRDF) of a metallic finish. Both ray tracing and hardware based rendering are demonstrated. In the latter case, we show how the calculation of a sphere map texture used for BRDF visualization can be accelerated using a special coordinate system for tabulated BRDF. The depth effect manifested by nashiji lacquer is simulated by the explicit modeling of metal platelets immersed in absorptive material.

Categories and Subject Descriptors (according to ACM CCS): I.3.7 [Computer Graphics]: Three-Dimensional Graphics and Realism

1. Introduction

From olden times lacquer work such as those shown in Fig. 1, commonly called *urushi*, has been used so widely for interior decoration, table ware and for other purposes that it is almost inseparable from the daily life of the Japanese. But *urushi* art of a highly artistic quality is inaccessible to the people in general, because the valuable materials, such as *genuine urushi* (lacquer juice), gold and silver, together with the skilled workmanship and the time required to make it, make its price almost prohibitive to them. However, in recent years cheap *urushi* art for utility purposes is being manufactured in large quantities for the use of the people who have a liking for anything new and novel. Because of this trend the merits of fine *urushi* art are gradually losing recognition.

Attracted by expressive beauty and richness of visual effects, which can be obtained using the old paints and techniques, we attempt to visualize the realistic appearance of *urushi* at interactive speeds. Realistic rendering of objects with complex optical properties, which change appearance with viewing and illumination directions, becomes of primary importance at early design stage and in electronic com-

merce. The specific properties of Makie technique include *flip-flop* visual color variation depending on viewing and illuminating directions while the properties of Nashiji technique include *depth* and *sparkling* effects. Very nice objects painted with very fine techniques consisting of mixtures of precious metals can be seen only in national museums. Since the production of such items took several years they can hardly be reproduced again. The other application of this research could be the computer-aided preservation of cultural heritage in digital form ².

The computer-aided preservation of cultural heritage is one of the recently popular topics in computer graphics, geometric modeling, and virtual reality communities. Specifically, G. Pasko et al. ^{19,23} made a great project called 'Virtual Shikki,' which is devoted to preservation of Japanese lacquer ware. Their work concentrates mostly on shape modeling using the implicit functions. Other related works to digital preservation of shape and texture of existing three-dimensional objects using the measurements and 3D scanning are the Digital Michelangelo project ¹⁶ and the Florentine Pieta project ¹.



Figure 1: Digital photographs of a jewelry box. Top: painted with makie urushi technique and Bottom: painted with nashiji urushi technique.

There have been many papers ^{7, 10, 22} related to the modeling of metallic and pearlescent paints in CG literature, which make it possible to simulate all the optical effects observed on urushi paints. Unfortunately, those methods require huge number of rays to obtain the good approximation of material radiance.

An approach for rendering the pearlescent and metallic appearance was proposed by S. Ershov et al. ⁹ where the BRDF is designed based on decomposing the paint layer into stack of sub-layers. Their method use the statistical approach for calculation of light scattering within the paint. However, their method does not focus on rendering itself.

The multi-image rendering algorithms such as light fields ¹⁵ and Lumigraphs ¹¹ can capture the light distribution within the bounded region of 3-D space. The price paid for calculated light field at any point is the assumption of constant illumination and computationally expensive preliminary processing of input data, which cannot be computed on the fly.

Because we are concerned with applications related to electronic commerce and preservation of cultural heritage, such as web based trade and virtual museums, we focus on a

hardware based rendering, in which visualization of metallic finishes in Japanese lacquer ware is done using a sphere map approach.

The sphere environment map was originally developed by Blinn and Newell ⁴ to interactively show specular reflection of distant environment. The idea was later elaborated by generalizing the BRDF ^{5, 12, 18, 20}.

Debevec ⁸ combined captured environment maps with synthetic objects to produce the renderings with both synthetic objects and image based environments. Unfortunately, this technique does not work at interactive speeds.

This drawback was overcome with hardware acceleration and image based rendering described by B. Cabral et al. ⁶. The authors used a sphere map which is view dependent representation. To avoid recalculation of the sphere map, the authors generate multiple sphere maps for different orthographic cameras. Afterwards, during the walk-through the sphere maps are interpolated using image based rendering (IBR) to ensure real time rendering. However, generation of reference sphere maps takes several tens minutes.

Our approach to real time rendering of objects with complex appearance, like Japanese lacquer ware items, includes online fast calculation of sphere maps. This widens the spectrum of possible applications to online ordering shape and design of lacquer ware items.

Although, the above mentioned rendering methods can handle many optical effects that occur in urushi paints, they will fail to correctly visualize the depth effects caused by small metallic flakes dipped in lacquer. We describe the explicit modeling method which simulates the sparkling appearance of nashiji.

The rest of the paper is organized as follows. Section 2 recalls the attainments on the urushi coating and decoration, in particular the makie and nashiji surface decoration techniques. Here we also summarize the most dominant optical effects that can be observed on the most urushi items. The BRDF representation using the adaptive grid and the fast calculation of the sphere map applicable to real time rendering of virtual urushi art items is described in Section 3. In Section 4 we propose the fast rendering technique of makie art drawings which can clearly demonstrate the metallic color shifts (flip-flop) effects. Two rendering methods of nashiji art techniques which can handle the *depth* and *sparkling* effects are derived in Section 5. Finally, we presents some results obtained using our approach and we conclude this paper.

2. The Urushi Coating and Decoration

The clear urushi is prepared from the sap of the lacquer tree by cutting the bark of tree. The cleared urushi from impurities is used for coating and decoration of the urushi art items mostly made of wood. The urushi art items are produced in three steps:

1. Preliminary coating where the rough wooden surface will be smoothed by applying of several layers of mostly dark or red urushi. At this step the substrate color is determined.
2. Finishing the surface to a smooth and glassy finish.
3. Decorative process, where the designs are drawn on a urushi ground by sprinkling the gold or silver powder over sticky urushi.

2.1. Makie: Sprinkling

Makie is the most famous surface decoration in urushi art technique. Patterns are painted with clear urushi or the red urushi and then the fine silver, gold and other metallic powders are sifted and adhered over the wet pattern to decorate the surface. The powders are sprinkled by means of bamboo or horn tubes covered with silk screen, as well as with a brush dusting.

There are many kinds of makie techniques differing mainly in what kind of urushi is used for pattern drawing and what kinds of powders are used.

2.2. Nashiji: Pear Skin Finish

A type of ground decoration, so termed because it recalls the speckled skin of the Japanese pear. It is created by lacquering the surface and while it is still wet the fine gold or silver powders or an alloy of gold and small amount of silver with a faint bluish green tinge are sprinkled over it. Subsequently after this dries, a coat of a thinner urushi is applied to fix the metal sparkles. The process is repeated to create multiple layers. Each layer has to be polished to a smooth glossy finish in such a way that the gold or silver sparkles remain still under the surface. Finally, the top varnish is made by repeatedly coated surface with transparent and yellowish lacquer.

2.3. Optical Effects of Makie

- **Flip-flop:** Makie urushi technique is a coating with complex optical behavior which includes *flip-flop* visual color variation depending on viewing and illuminating directions. The color variation is usually the smooth visual variation between two colors. Optical behavior of such paints is mostly described by a bi-directional reflectance distribution function.

Other effects observed include the Fresnel reflections on solid paint.

2.4. Optical Effects of Nashiji

- **Sparkling:** An impressive phenomenon that can be observed in Nashiji lacquer ware is the *sparkling* effect caused by large metallic flakes. Under direct illumination the flakes become visible as tiny shining mirrors¹⁷. When

observed from far distance, the sparkles get blurred due to the finite resolution of human eye and one can observe a texture with irregular random fluctuations of brightness.

- **Depth:** As a result of sparkling the observer can get an impression of a very thick paint with the gold sparkles laying very deeply in it. The thickness impression can range from 3 ~ 5mm but the actual paint thickness could be less than 1mm as in Fig. 2.



Figure 2: An example of nashiji urushi item in which the depth effect is perceived.

3. BRDF Visualization

The focus of this paper is on real time visualization of real items in virtual world showing the complex optical effects during the walk-around the artistic item. The real-time BRDF visualization is needed for this purpose. This problem is solved by proposed coordinate system for BRDF representation adjusted to a method of fast calculation of a sphere map as described below.

3.1. BRDF Representation

The BRDF of a metallic urushi surface is directional diffuse; that is, such a BRDF exhibits fairly sharp change near the specular direction. We have measured BRDFs using the setup described by Letunov et al.¹⁴.

The tabular representation of BRDF using the spherical coordinate system (ψ, ξ) with polar axis along the surface normal and a uniform grid of points does not provide good accuracy in a specular peak area, unless the grid density is very high, up to hundred thousand of tabular entries. The BRDF is represented in this system as $f(\psi_i, \xi_i, \psi_o, \xi_o)$, where

$$\vec{n} = \text{Surface normal,}$$

$$\vec{\omega}_i = (\psi_i, \xi_i) \text{ is incident direction relative to } \vec{n},$$

$$\vec{\omega}_o = (\psi_o, \xi_o) \text{ is outgoing direction relative to } \vec{n}.$$

The similar problems related to BRDF representation were considered by Rusinkiewicz²¹. He uses the parameterizing the BRDF in terms of the halfway vector between the incoming and outgoing rays and a *difference* vector. We will consider the BRDF in terms of the specular direction and a local vector.

We can decrease the size of the discretized BRDF stored in a table to several hundred entries. Each value in a table

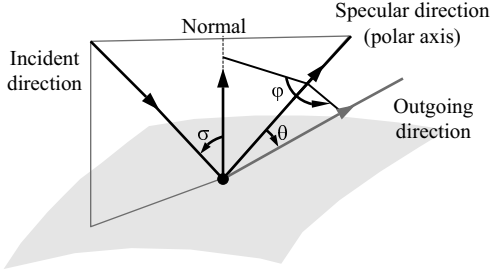


Figure 3: BRDF representation. A special coordinate system for BRDF representation.

is associated with the discrete coordinates (θ, ϕ) , of a rotated spherical coordinate system with the polar axis along the specular direction, as shown in Figure 3. The BRDF is represented in this system as $f(\theta_i, \phi_i, \theta_o, \phi_o)$, where

$$\begin{aligned} \vec{s} &= \text{Specular direction,} \\ \vec{\omega}_i &= (\theta_i, \phi_i) \text{ is incident direction relative to } \vec{s}, \\ \vec{\omega}_o &= (\theta_o, \phi_o) \text{ is outgoing direction relative to } \vec{s}, \\ \theta_o(\psi, \xi) &= \text{Angle between } \vec{\omega}_o \text{ and } \vec{s} \text{ directions,} \\ \phi_o(\psi, \xi) &= \text{Angle around } \vec{s}. \end{aligned}$$

As a result of this parameterization a sharp peak of diffuse BRDF will be in predefined area of BRDF domain around the polar axis in a new coordinate system. We can then discretize the BRDF and adjust the grid density making it more dense for small values of θ , in other words grid will be dense near the specular peak and sparse in the areas far from polar axis.

This method provides a high and almost uniform accuracy of approximation and does not need as many grid points as it would be necessary for an uniform grid.

3.2. Sphere Map Generation

The *sphere map*, shown in Fig. 4, is an image resulting from an orthographic projection of a sphere whose surface BRDF matches that of the target object. The sphere is rendered for the same illumination and observation conditions as for target object.

Next we restrict ourselves to the case of several directional light sources and distant point light sources. Therefore, calculating the lighting equation for the sphere radiance map ⁶ amounts to the classic ray tracing of the sphere.

To render a sphere map, we select a pixel from sphere map, shoot a ray from the camera through this pixel, and find where it hits the sphere. At this point, we fire rays to all light sources and calculate the radiance from the sphere BRDF, the local normal, the viewing and illumination directions as

$$L(\vec{\omega}_o) = \sum_k f(\vec{\omega}_{ik}, \vec{\omega}_o) I_k(\vec{\omega}_{ik}),$$

where L is the radiance in the $\vec{\omega}_o$ outgoing direction, f is the BRDF, I_k is the incident radiance of the sphere at the point hit by the ray, coming from the k -th light source, $\vec{\omega}_{ik}$ is the direction to the k -th light source.

3.3. Fast Re-calculation

If we could create a good mesh on the sphere and shade only few vertices of the mesh and then interpolate all other points, the sphere map generation could be extremely fast. Furthermore, the color interpolation between mesh points can be done in hardware with Gouraud shading.

Below we will focus on the problem of construction of a good mesh for a single light source. To obtain the sphere map for several light sources, we just repeat the whole process for each light source and superimpose the sphere maps using the blending operation.

Looking at a "typical" sphere map image, shown in left of Fig. 4, for a single light source we see that a fixed polar or rectangular mesh will not be optimal, because, like for BRDF, there is a small area with large intensity gradients where the mesh must be fine and a large area with small gradients where we can use a coarse-grained mesh.

An optimal mesh should follow the BRDF changes. The BRDFs for metallic paints have a very strong dependence on angle θ in our BRDF representation, refer to Figure 3. Therefore, the best choice is the mesh with parametric lines along which the angle θ is constant, i.e. $\theta(\psi, \xi) = C_\theta$. The second family of parametric curves is naturally drawn from the highlight center along the constant angle ϕ , i.e. $\phi(\psi, \xi) = C_\phi$. The points (ψ, ξ) refer to the spherical coordinates relative to the \vec{n} on the rendered sphere. Unfortunately, such mesh is not uniform along the ellipsoidal curves for constant θ . The mesh is improved by discrete arc-length reparameterization of parametric curves $\theta(\psi, \xi) = C_\theta$.

The resulting mesh derived for a measured BRDF of a gold metallic paint is shown in Figure 4 on right. If the number of light sources is no larger than ten, the time needed for calculation of a sphere map with our approach is a few tens of milliseconds for Pentium III machines with contemporary video cards.

4. Makie Simulation

This section describes preprocessing of the lacquer digital image to obtain information about distribution of colored urushi, metallic finish, and hardware based rendering of the makie lacquer ware.

4.1. Acquiring Optical Information

The surface of a makie item is usually painted with one, two or three types of colored urushi and one type of metallic finish. We prepare samples for each of the types of colored urushi used in the item under study. In particular, we

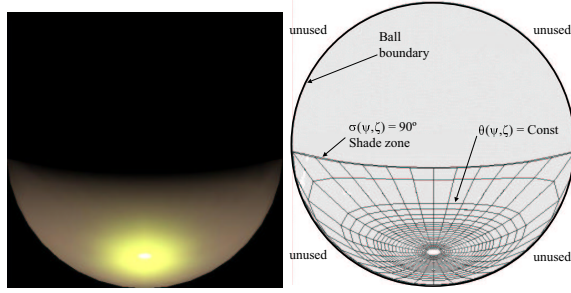


Figure 4: Sphere map. Left: Sphere map of a gold metallic paint. Right: Mesh for fast calculation of a sphere map.

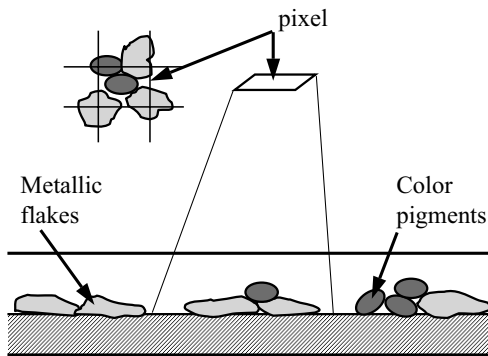


Figure 5: Cross section of the makie urushi showing pixel covering the sample.

make a metallic finish sample where platelets are sprinkled in such a density that no free space between them remains. We make photos of these samples under the same illumination conditions as that of the item. Because illumination should not vary significantly over the place where the art item or samples are put, it is best to use daylight illumination. We then extract radiometric information in the form of a high dynamic range (HDR) image from photos of the item and samples using Debevec's approach at <http://www.debevec.org/Research/HDR/>. If there is no too bright or too dark pixels on the image, then simple gamma transformation is enough. This is because CCD matrices are highly linear, so nonlinearity is added by the camera circuitry at the output, and this nonlinearity is only often gamma correction - at least, in some range of medium luminances. Further calculations are done either in XYZ or any RGB space, such as that of the camera after gamma transformation, obtained from CIE XYZ by a linear transformation.

Colored urushi paints are not intermixed on makie; different types of it are applied on different places. The color of each colored urushi varies over its patch only slightly because the application conditions such as, the layer thickness vary only slightly. On the other hand, the metal component of the finish consists of small thin (micrometers) platelets

glued to the surface of colored urushi. In some types of urushi, pigment particles are also glued on the colored urushi after metal particles have been sprinkled on it. Figure 5, shows how sprinkled metal particles of makie are covered by a pixel of a CCD matrix in a digital camera. As a result, the colors of metallic and pigmented finishes mix additively rather than subtractively. This means that if metallic platelets occupy some fraction p of the colored urushi surface, then the BRDF f is a weighted sum of the BRDF of the metallic finish $f_{metallic}$ and those of colored urushi:

$$f = pf_{metallic} + \sum_l q_l f_l,$$

with p, q_l being positive scalar weights, f_l is the BRDF of the l -th colored urushi, and q_l is the fraction of the surface occupied by it. More general approach was considered by Lensch¹³ were they used the image-based measuring method for BRDFs. We will consider $f_{metallic}$ as given from measurements and all other basis elements and weight must be estimated.

We assume that the BRDF of small patches of metallic finish, including individual platelets, is the same as that of a large patch consisting of platelets glued to the lacquer surface without gaps. This assumption is justified by the following facts:

1. Metallic platelets are glued practically in one layer.
2. They are well aligned with the lacquer surface so light interreflections between neighboring platelets are negligible.

Similarly, we assume that the BRDF of a small patch covered with glued pigment particles used in a colored urushi is the same as that of a large patch. For colored urushi, this assumption is less justified, because two above facts are not true for them. But the BRDF of colored urushi is close to a Lambertian one plus the Fresnel reflection from the outer pigment-free layer, so differences between the BRDFs for small and large areas are not so important.

4.2. Selection the f_l Basis and Coefficients

Given the BRDFs, the radiance of a pixel in HDR image can be calculated as the BRDFs summed with lighting and integrated over the surface area covered by the pixel projection. Therefore, the radiance for three color channels is

$$\mathbf{T}(i, j) = p(i, j)\mathbf{m} + \sum_l q_l(i, j)\mathbf{c}_l, \quad (1)$$

where \mathbf{m} and \mathbf{c}_l are color triplets of a surface covered by only metallic finish and by only the l -th colored urushi, respectively. Therefore, positive weight are constrained by $p + \sum_l q_l = 1$ at pixels in drawing and $p + \sum_l q_l < 1$ at boundary pixels. Our goal is to find $p(i, j)$ and $q_l(i, j)$.

To this end, we change the basis of the three-dimensional color space used in such a way that \mathbf{c}_l become basis vectors. At this point, we recall that most makie items have no

more than three types of colored urushi. If we assume exactly three, then a new basis has three vectors collected in a matrix

$$A = (c_1 c_2 c_3).$$

At this point, we assume that the HDR color of metallic finish \mathbf{m} is contained in the convex hull of basis vectors \mathbf{c}_l , $l = 1, 2, 3$. Usually, this is so because \mathbf{c}_l are either some red, green and blue colors or some red, green and white colors, while \mathbf{m} is goldish.

Therefore, by multiplying the Eq. 1 from left side with inverse matrix A^{-1} we have the equation in new basis

$$\mathbf{T}'(i, j) = p(i, j)\mathbf{m}' + \sum_{l=1}^3 q_l(i, j), \quad (2)$$

where

$$\begin{aligned} \mathbf{T}' &= (T'_1, T'_2, T'_3) = A^{-1}\mathbf{T}, \\ \mathbf{m}' &= (m'_1, m'_2, m'_3) = A^{-1}\mathbf{m}, \end{aligned} \quad (3)$$

and \mathbf{m}' is the triplet color of the metallic finish with respect to the new basis.

Now we recall that colored urushi patches are not inter-mixed. Therefore, if we knew the fraction of metallic finish for each pixel p exactly, we would find that, in the limit of infinitesimally small pixels, only one of q_l should be nonzero for any pixel. In reality, because the color of colored urushi \mathbf{c}_l is not absolutely constant and two or three color patches may meet at a pixel, more than one q_l are nonzero. But, for most pixels, we have the largest q_l for the colored urushi that is actually present in the area covered by the pixel and other weights are small or zero.

Noting that q_l are positive, we can approximately find $p(i, j)$ as

$$p(i, j) = \min\{T'_1(i, j)/m'_1, T'_2(i, j)/m'_2, T'_3(i, j)/m'_3\}. \quad (4)$$

The obtained $p(i, j)$ values are actually the alpha values of the generated texture shown on top-right of Figure 6. The second term of Eq. 2 after linear transformation to the monitor RGB is the RGB residual texture shown on bottom of Figure 6. The alpha component and the RGB image form the final RGBA texture.

4.3. Rendering Makie and Colored Urushi

Our approach employs a texture for rendering the Lambertian reflectance of colored urushi (see bottom of Fig. 6) and sphere map texture (see Section 3) for visualization of measured BRDF of metallic (gold or silver) finish. For controlling the ratio between two types of reflectances, we use the alpha channel of the texture calculated from Eq. 4. Thus, in our implementation we render objects of arbitrary geometry using multitexturing method, one texture mapping uses

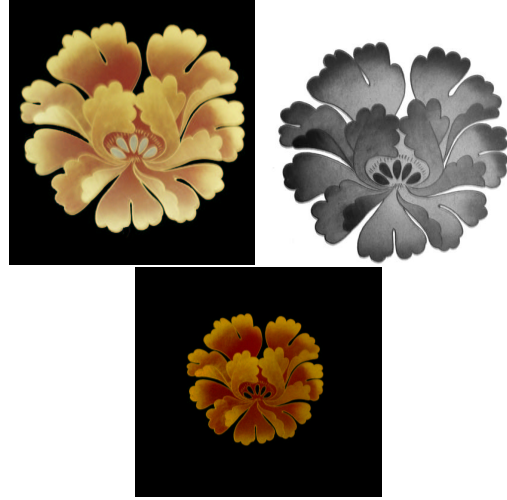


Figure 6: Texture decomposition. Left: Digital photo of a pattern. Right: Alpha channel used for weight of metallic BRDF. Bottom: Pattern without the metallic components.

the metallic sphere map and the other one is ordinary texture mapping with residual texture. The two texture images are then blended together according to the alpha channel.

The artistic drawing should be captured from flat areas for correct mapping to more complex geometries. The rendering runs in real time with different geometries.

5. Nashiji Depth Effect Simulation

There are many mechanisms responsible for perception of the depth effect produced by sparkles. One such mechanism called rivalry is the result of competition between images perceived by the left and right eyes. This mechanism can be demonstrated when one eye look at black and the other eye on white circle. The result of perception is gray and later it will continually change between white and black circles.

The similar mechanism can be present when looking at sparkles. The same flake can be seen bright by one eye and dark by the other one. As a result of rivalry perception mechanism we will perceive the depth effect.

We can simulate this effect by explicit modeling of the geometry of sparkles distributed along the geometry of the shape. The sparkles are defined as implicit superquadric functions³. The reason why we use the implicit functions is that they need less number of parameters to be defined thus saving the memory. For the simplicity, we assume that all sparkles have the same given shape. Their distribution, density and orientation is random according to the the user defined distribution functions. All flakes have the metallic finish and are immersed in the absorption media given by absorption coefficients for each RGB color channel.



Figure 7: Stereo pair showing the sparkling depth effect.

Visualization of such complex scene is done by raytracing method yielding a stereo pair of images as shown in Fig. 7. The stereo visualization enables to simulate the rivalry perception mechanism. The explicit modeling of geometry sparkles has the advantage that we can freely zoom in and out while the sparkling patterns will change smoothly during the walk-around animations.

6. Results

The proposed method for Makie visualization have been implemented as our real-time visualization system using Java3D. Users can observe the color shifts by rotating the object in real time as can be seen in Figure 8.



Figure 8: Makie rendering at different view angles.

Figure 9* shows a frame from an animation of a Japanese cup on tray showing the color changes of simulated makie technique the flip-flop effect.

For nashiji simulation, we have implemented the modeling tool for distribution of explicitly defined flakes over a parametric shape. Unfortunately, the raytracing of sparkles is computationally a heavy task, we leave the improvement of this method as the future research.

7. Conclusions

We have described new methods with focus on real time visualization of real artistic items in virtual world showing the complex optical effects. We consider two most popular kinds of Japanese lacquer ware made by the makie and nashiji techniques. We described interesting optical effects that can be observed in both techniques, which can be simulated by the proposed methods.

The real-time BRDF visualization method based on color interpolation between the vertices of an adaptive mesh on sphere map image was developed.

The depth and sparkling affects observed mostly on nashiji urushi technique were visualized by proposed explicit modeling of metallic flakes, which enable the user to smoothly zoom in and out the object surface and observe the depth effect in an image stereo pair. However, we left as future work the extension of our explicit sparkling technique to handle calculations in real time.

Acknowledgements

The author wishes to thank Dr. S. Czanner for nice photographs of urushi, R. Kimura and S. Kato for preparing the models and rendering the animation, Dr. A. Letunov for measuring urushi samples and Dr. A. Fujimoto, Prof. K. Myszkowski and Prof. W.L. Martens for fruitful discussions about the color perception effects during course of this work. This research was sponsored by grants from the Fukushima Prefectural Foundation in Japan for the Advancement of Science and Education.

References

1. J. Abouaf. The Florentine Pieta: Can visualization solve the 40year-old mystery? *IEEE Computer Graphics and Applications* **19**(1):6–10, 1999. 1
2. A. Addison and Y. Le Lous. Emerging trends in virtual heritage. *IEEE Multimedia, Special Issue on Virtual Heritage*, **7**(2):22–25, 2000. 1
3. A.H. Barr. Superquadrics and angle-preserving transformations. *IEEE Computer Graphics and Applications*, **1**(1):11–23, 1981. 6

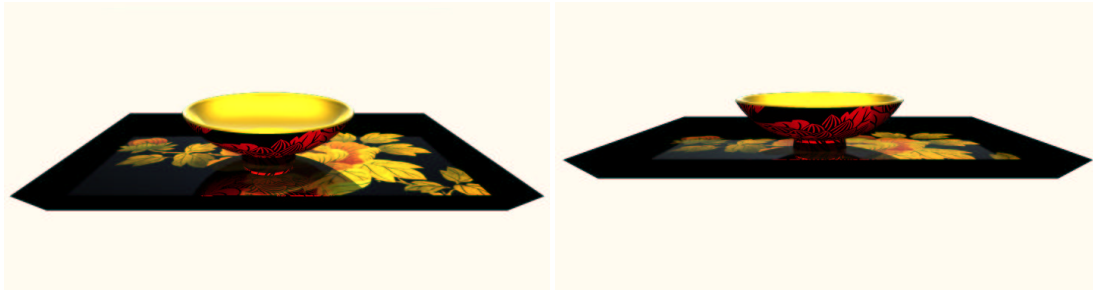


Figure 9: Animation sequence.

4. J. Blinn and M. Newell. Texture and reflection in computer generated images. *Communications of the ACM*, **19**:542–546, 1976. 2
5. B. Cabral, N. Max and R. Springmeyer. Bidirectional reflection functions from surface bump maps. In *Computer Graphics (SIGGRAPH '87 Proceedings)*, M. C. Stone, Ed., **21**, 273–281, 1987. 2
6. B. Cabral, M. Olano, and P. Nemeč. Reflection space image based rendering. *Proceedings of SIGGRAPH 1999*, ACM SIGGRAPH, 165–169, 1999. 2, 4
7. K.J. Dana, B. van Ginneken, S.K. Nayar, and J.J. Koenderink. Reflectance and texture of real-world surfaces. *ACM Transactions on Graphics* **18**(1):1–34, 1999. 2
8. P. Debevec. Rendering synthetic objects into real scenes: Bridging traditional and image based graphics with global illumination and high dynamic range photography. *Proceedings of SIGGRAPH 1998*, ACM SIGGRAPH, 189–198, 1998. 2
9. S. Ershov, K. Kolchin, and K. Myszkowski. Rendering pearlescent appearance based on paint-composition modelling. *Computer Graphics Forum* **20**(3):C221–C238, 2001. 2
10. J.S. Gondek, G.W. Meyer, J.G. Newman. Wavelength dependent reflectance function. *Proceedings of SIGGRAPH 1994*, ACM SIGGRAPH, 213–220, 1994. 2
11. S.J. Gortler, R. Grzeszczuk, R. Szeliski, and M.F. Cohen. The Lumigraph. *Proceedings of SIGGRAPH 1996*, ACM SIGGRAPH, 43–54, 1996. 2
12. N. Greene. Applications of world projections. In *Proceedings of Graphics Interface '86*, M. Green, Ed., 108–114, 1986. 2
13. S.M. Rusinkiewicz. Image-based reconstruction of spatially varying materials. *Proceedings of Eurographics Workshop on Rendering*, 95–103, 2001. 5
14. A.A. Letunov, B.H. Barladian, E.Yu Zueva, V. Vezhn-evets, and S. Soldatov. CCD-based device for BRDF measurements in computer graphics. *Proceedings of Graphicon 99*, August 26 - September 1, Moscow, 129–138, 1999. 3
15. M. Levoy and P. Hanrahan. Light field rendering. *Proceedings of SIGGRAPH 1996*, ACM SIGGRAPH, 31–42, 1996. 2
16. M. Levoy et al. The digital Michelangelo project: 3D scanning of large statues. *Proceedings of SIGGRAPH 2000*, ACM SIGGRAPH, 131–144, 2000. 1
17. S.C. McCamy. Observation and measurement of the appearance of metallic materials. Part I. Macro appearance. *COLOR research and application*, **21**:292–304, 1996. 3
18. G. Miller and C. Hoffman. Illumination and reflection maps: Simulated objects in simulated and real environments. In *SIGGRAPH '84 Advanced Computer Graphics Animation seminar notes*, July 1984. 2
19. G. Pasko, A. Pasko, C. Vilbrandt, and T. Ikedo. Virtual Shikki: Shape Modeling in Digital Preservation of Traditional Japanese Lacquer Ware. *Proceedings of the 17th Spring Conference on Computer Graphics*, Editors R. Ďurikovič and S. Czanner, IEEE Computer Society, April 25–28, Budmerice, Slovakia, 147–154, 2001. 1
20. P. Poulin and A. Fournier. A model for anisotropic reflection. In *Computer Graphics (SIGGRAPH '90 Proceedings)*, F. Baskett, Ed., **24**, 273–282, 1990. 2
21. S.M. Rusinkiewicz. A new change of variables for efficient BRDF representation. *Proceedings of Eurographics Workshop on Rendering*, 11–22, 1998. 3
22. M. Schramm, J. Gondek, and G. Meyer. Light scattering simulations using complex subsurface models. *Proceedings of Graphics Interface 1997*, 56–67, 1997. 2
23. WEB page: Virtual Shikki Web site. URL: <http://www.k.hosei.ac.jp/~pasko/Shikki/Shikki.html> 1